

Recent results on nucleon electromagnetic form factors at BESIII

F. De Mori on behalf of BESIII collaboration

Dip. di Fisica dell'Università degli Studi di Torino e INFN sez. di Torino, via P. Giuria 1, 10126 Torino, Italia.

Received 20 December 2021; accepted 29 January 2022

We report recent results of nucleon electromagnetic form factors at the BESIII experiment. The BESIII detector is installed at the BEPCII electron-positron collider in Beijing (PRC) with a center-of-mass energy range between between 2.0 and 4.9 GeV. The nucleon electromagnetic form factors has been measured in BESIII both via direct e^+e^- annihilation and initial-state-radiation technique.

Keywords: QCD; nucleon structure; electromagnetic form factors.

DOI: <https://doi.org/10.31349/SuplRevMexFis.3.0308083>

Electromagnetic form factors (FFs) provide information on the internal structure and dynamics of hadrons, describing the modifications of the point-like photon-hadron vertex due to the hadron structure and allow a better understanding of the strong interaction.

Their number is related to the spin of the hadron of spin S as $(2S+1)$.

Therefore, for the direct annihilation process in two nucleons in one photon exchange approximation, two FFs are needed to describe the hadronic vertex, shown in Fig. 1, as

$$\Gamma^\mu(q^2) = \gamma^\mu F_1(q^2) + i \frac{\sigma^{\mu\nu} q_\nu}{2m} F_2(q^2), \quad (1)$$

where F_1 and F_2 are the so-called Dirac and Pauli FFs and m is the mass of the corresponding nucleon. FFs, in the Breit system, represent the Fourier transforms of electric charge and magnetization spatial distributions of nucleons.

The Sachs parametrization, in which the FFs are linear combinations of F_1 and F_2 , is widely used, written as

$$\begin{aligned} G_E(q^2) &= F_1(q^2) + \frac{q^2}{4m^2} F_2(q^2), \\ G_M(q^2) &= F_1(q^2) + F_2(q^2). \end{aligned} \quad (2)$$

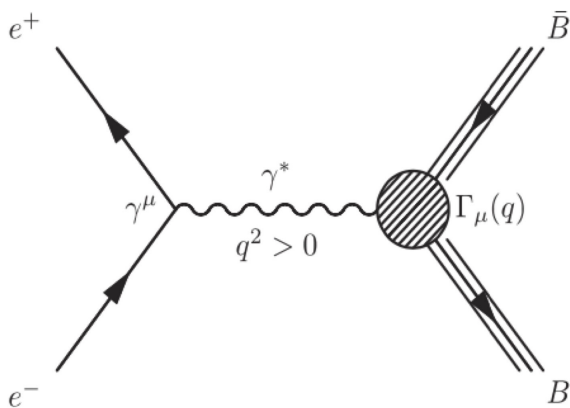


FIGURE 1. Lowest-order Feynman diagram for the annihilation process $e^+e^- \rightarrow B\bar{B}$.

As an example, proton FFs can be measured in different kinematic regions by lepton-proton elastic scattering (space-like, SL) and electron-positron annihilation into a proton-antiproton pair or proton-antiproton annihilation into an electron-positron (time-like, TL). They bring different and complementary pieces of information. The FFs are analytic functions of the momentum transfer squared q^2 and they are real in the space-like region ($q^2 < 0$) and complex in the time-like region ($q^2 > 0$), above the production threshold, due to the unitarity. The analytic structure of the TL FFs is connected by dispersion relations to the SL regime. Measurements in different kinematical regions allow rigorous test of perturbative QCD and phenomenological models. Up to now the knowledge of the TL proton FF is rather limited with respect to the SL sector, where a percent level precision was achieved [1].

Indeed, in one-photon exchange approximation, the Born differential cross section in the e^+e^- c.m. and the total cross section can be written, parameterized by both the FFs, as

$$\begin{aligned} \frac{d\sigma^{\text{Born}}}{d\Omega}(q^2, \theta_B) &= \frac{\alpha^2 \beta C}{4q^2} \left((1 + \cos^2 \theta_B) |G_M(q^2)|^2 \right. \\ &\quad \left. + \frac{1}{\tau} \sin^2 \theta_B |G_E(q^2)|^2 \right) \end{aligned} \quad (3)$$

and

$$\sigma^{\text{Born}}(q^2) = \frac{4\pi\alpha^2\beta C}{3q^2} \left(|G_M(q^2)|^2 + \frac{1}{2\tau} |G_E(q^2)|^2 \right), \quad (4)$$

where θ_B is the polar angle of the baryon, $\tau = q^2/4m^2$, $\beta = 1 - 1/\tau$ and the Coulomb factor C accounts for the electromagnetic interactions of point-like baryons, crucial at threshold, and is equal to 1 for neutral baryon pairs [2].

In the past, due to the low statistics, only the so-called effective FF, G_{eff} , could be determined, written as:

$$|G_{eff}| = \sqrt{\frac{|G_E|^2 + 2\tau |G_M|^2}{1 + 2\tau}}. \quad (5)$$

It can be determined from the total cross section, under the assumption $|G_E| = |G_M| = |G_{eff}|$, that is implied by analyticity at threshold.

Concerning the Initial State Radiation (ISR) technique, the total cross section can be factorized, disentangling the reaction of interest from the radiator function $W(x, s)$, which gives the probability of emission of a hard photon and depends on its energy and angle.

The differential cross section of the ISR process $e^+e^- \rightarrow p\bar{p}\gamma$ and the radiator function read as

$$\frac{d\sigma_{p\bar{p}\gamma}}{dq^2}(q^2) = \frac{1}{s}W(s, x)\sigma_{p\bar{p}}(q^2),$$

$$W(x, s) = \frac{\alpha}{\pi x} \left(\ln \frac{s}{m_e^2} - 1 \right) (2 - 2x - x^2), \quad (6)$$

being $x = 2E_\gamma^*/\sqrt{s}$, with E_γ^* the energy of the ISR photon in the e^+e^- c.m. frame, \sqrt{s} the center of mass energy and m_e the electron mass.

This method allows to scan large q^2 intervals with fixed energy (\sqrt{s}) colliders and the loss of cross section is largely compensated by the high luminosity of the machines.

Moreover, with both methods, the ratio of the electric and magnetic FFs, $R_{em} = |G_E/G_M|$, is experimentally accessible by the measurement of the differential cross section at a given q^2 . In principle a precise measurement of the differential cross section would allow to disentangle the FFs' moduli, *i.e.* the electric, $|G_E|$ and the magnetic, $|G_M|$.

1. BESIII

The BESIII spectrometer is installed at the high luminosity, multi-bunch BEPCII electron-positron collider. The design luminosity of $10^{33} \text{ cm}^{-2} \text{ s}^{-1}$ was reached in 2016 at a center-of-mass energy of 3.78 GeV.

It covers 93% of full solid angle. Details of each sub-detector and their performance, together with the trigger system, are discussed in Ref. [3].

The BESIII detector has been operating since 2009, collecting unique data samples. Its main components are: a Multi-layer Drift Chamber (MDC), a Time-of-Flight (TOF) system, an Electromagnetic Calorimeter (EMC) and a Muon Counter (MUC). A superconducting solenoid magnet provides 1.0 T magnetic field. The experiment has received several upgrades, and new upgrades for both the detector and accelerator are foreseen.

In BESIII, with electron-positron annihilation, both energy scan and the ISR techniques can be applied to measure time-like FFs.

2. Recent results on Proton FFs

BESIII obtained results from four different analyses. The last scan-method analysis [4] accounts for all the available high statistics data set between $\sqrt{s} = 2.2$ and 3.08 GeV with 22 energy points, corresponding to a total integrated luminosity of 669 pb^{-1} .

Two analyses used ISR technique with two different approaches, called Small Angle-ISR (SA-ISR) or untagged and

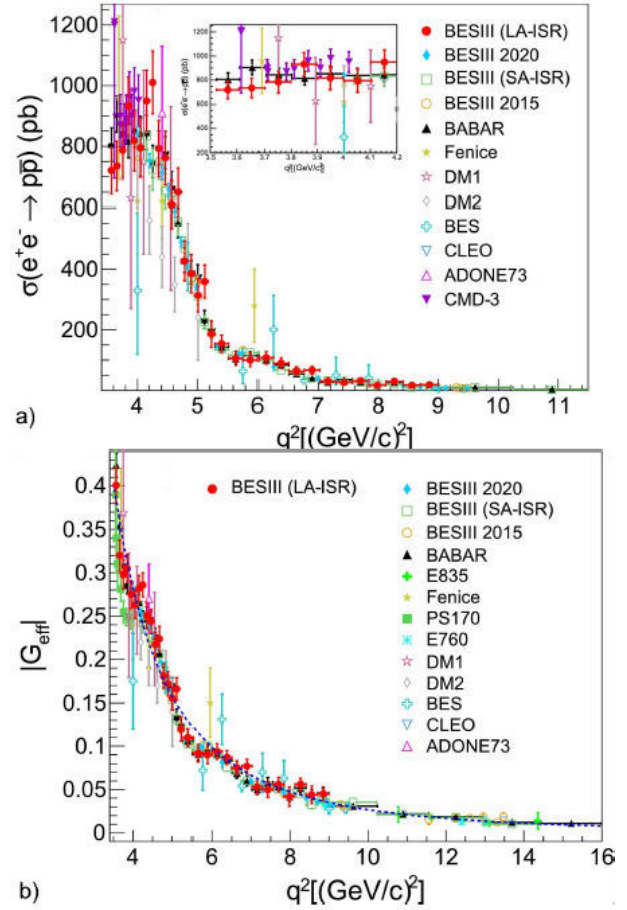


FIGURE 2. Latest BESIII results (red points) including statistical and systematic uncertainties for the Born cross section on the top (a) while on the bottom (b) the $|G_{eff}|$ with a fit through the data (blue dashed line) with previously published measurements (references in [4]).

Large Angle-ISR (LA-ISR) or tagged, in which angle refers to the polar angle of the ISR photon.

The untagged ISR analysis [5] exploits $e^+e^- \rightarrow p\bar{p}\gamma$ events in which the ISR photons cannot be detected by the EMC with a statistics increased by a factor 3 compared to the tagged analysis. These two independent analyses are based on the same collected data sets but with complementary samples. A integrated luminosity of 7.5 fb^{-1} between $\sqrt{s} = 3.773$ and 4.6 GeV was used. By tagged ISR measurement [6] the Born cross section and the effective FF of the proton are measured from the production threshold to 3.0 GeV. Although the signal/background separation is more complicated, using the information of just two detected particles, this method represents the only way to reach the threshold, with a valuable harvest. Indeed, this region presents a special interest because of its peculiar features not yet understood.

In Fig. 2, the experimental measurements of the Born cross section σ_B a) and effective FF G_{eff} b) can be found as a function of the momentum transfer squared for all BESIII analyses and the other measurement available in litera-

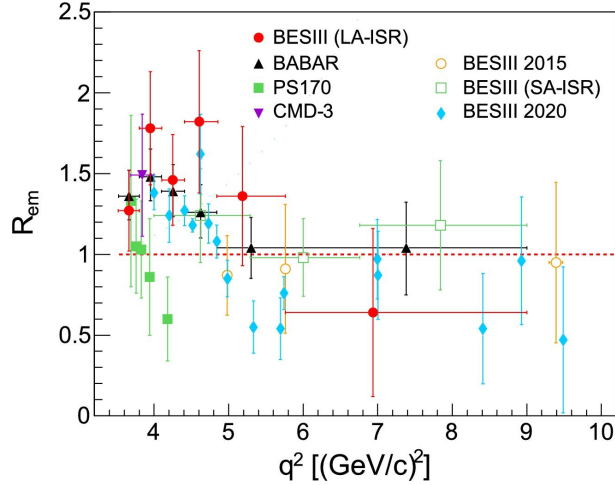


FIGURE 3. Tagged ISR BESIII Results (red points) for $|R_{em}|$ as a function of the momentum transfer squared, q^2 , together with the results from previous experiments.

ture. The wider momentum transfer range can be appreciated in comparison with the previous ones. We confirm previous measurements with the two-three step behavior in the cross section, most likely due to final state interactions. In particular, it is important to notice that the behavior at threshold, shown in the insight of Fig. 2a) and measured by BaBar with lower uncertainties, is confirmed even if our LA-ISR measurements seem to be systematically lower. The effective FF distribution show a steep behavior at threshold as confirmed by our LA-ISR analysis, that can reach the threshold, as can be appreciated in Fig. 2b). It is well described by a modified dipole function shown as a blue dashed line, phenomenologically motivated [7]. More details will be found in the next section. However, oscillating structures are clearly seen when the residuals are plotted as a function of the relative momentum p of the final proton and antiproton.

From the analysis of the proton-helicity angular distribution, the ratio of electric and magnetic ($|R_{em}|$) FFs of the proton is determined. Close to the threshold, the observed ratio is compatible with unity within the uncertainties. These BESIII measurements confirm an enhancement of $|R_{em}|$ in the region below $2.2 \text{ GeV}/c^2$ previously observed by BaBar and differs from the behavior reported by PS170, not obtained in e^+e^- annihilation though. This shed light towards the solution of the long-standing significant discrepancy. The available full proton angular distribution allows to reach better precision of the ratio of FFs.

The dotted line represents pQCD asymptotic prediction and nucleon final state interactions can account for deviations for $q^2 < 5 \text{ GeV}^2$. Moreover, BESIII was able, thanks to its high statistics, to measure, for the first time, $|G_E|$ and $|G_M|$ independently.

Furthermore it obtained the most precise results for $|G_M|$ and $|R_{EM}|$ with a relative precision of 1.8% - 3.6% and 3.5% - 96%, respectively. The scan-method analysis allows the measurement over a wide q^2 range, that is an important achievement. BESIII results bring new information with a

comparable precision to the scattering region and helps going towards a unified view of the scattering and annihilation regions.

3. Recent results on Neutron FFs

The high integrated luminosity collected with BESIII between $\sqrt{s} = 2.0$ and 3.08 GeV , represents a unique opportunity for a precise measurement of the neutron FFs in the process $e^-e^+ \rightarrow n\bar{n}$. Because of the difficulties in the (anti-)neutron detection, only a few measurements were available, obtained by the three experiments: FENICE [10], DM2 [11] and SND [12]. Indeed these challenging measurements have been awaited since long time. In the meanwhile this allows both the comparison with proton FF measurements and between available data in Space-Like and Time-Like regions.

In our analysis [13] three statistically independent event categories are used to maximize the reconstruction efficiency of the $n\bar{n}$ final state, depending on the interaction of the (anti-)neutrons with the detector. Neutron/anti-neutron candidates are selected using informations from EMC and/or

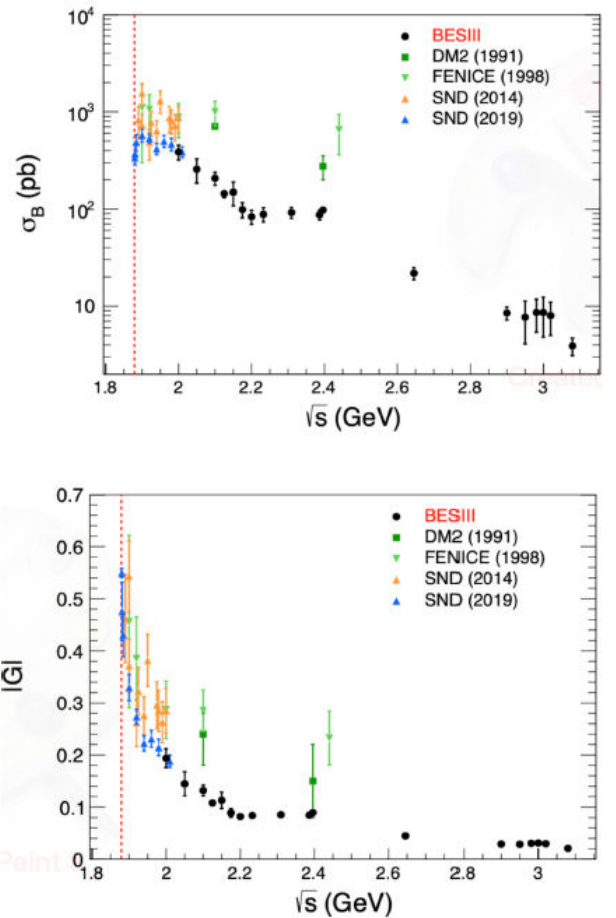


FIGURE 4. Results for the Born cross section (top) and the corresponding FF $|G_{eff}|$ (bottom) for the $e^-e^+ \rightarrow n\bar{n}$ for BESIII (black solid circles) and FENICE [10], DM2 [11], and SND [12] experiments. The red dashed line indicates the production threshold.

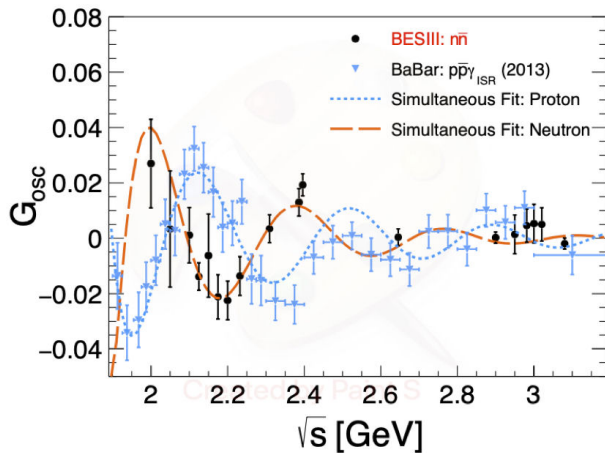


FIGURE 5. The reduced FF G_{osc} of the nucleon, as defined in the text, is shown as a function of the relative momentum of the nucleon pair for BESIII data for neutron (black circles) and BaBar data for proton (blue triangles) [14] with the simultaneous fit.

TOF only, because no Hadronic Calorimeter is available. The signal yield is obtained after subtracting the residual background beam-related or caused by cosmic ray, multi-hadronic and di-gamma processes. The results from the three categories are consistent with each other and were combined to reduce the statistical uncertainty.

The cross section of the process is measured at 18 c.m. energies, obtaining the best precision of 8.1% at $\sqrt{s} = 2.396$ GeV. Then the effective FFs are extracted under the assumption $|G_E| = |G_M|$ with an improvement of the statistical precision improved by more than a factor of 60 over previous measurements from the FENICE and DM2 experiments. The results are shown in Fig. 4. Here it is evident the importance of our measurements for its wide range and very low uncer-

tainties, starting to be competitive with SL ones. They agree with SND and FENICE at 2.0 GeV, but above 2.0 GeV they are systematically lower.

After the subtraction of the dipole-like function [7], the reduced FF can be described by the following function,

$$G_{osc}(p) = A \exp(-Bp) \cos(C \cdot p + D) \quad (7)$$

where p is the relative momentum of the nucleon pair, A the normalization, B the inverse oscillation damping, C the momentum frequency, and D the phase. A fit to the proton and neutron data can simultaneously describe the oscillation with a phase shift of $(125 \pm 12)^\circ$, as shown in Fig. 5. This is most likely sign of a more complex dynamic effect, which still needs clarification, like interference effects in final state re-scattering [8] or presence of resonances in the data [9].

Moreover the preliminary BESIII results for $|G_M|$ can be compared to the results from FENICE, extracted from the Born cross section using the hypothesis $|G_E| = 0$. They are significantly larger compared to BESIII.

4. Conclusions

The BESIII experiment is ideal to measure the nucleon FFs in the time-like region. With the large data sets collected, the precision of the effective FFs of the proton and the neutron is increased with respect to previous experiments. The magnetic and electric FFs of the proton are measured independently for the first time and $|R_{em}|$ is measured with improved precision. An oscillating behavior of the effective FF is observed both for neutron and proton. Larger samples, that BESIII is collecting, will improve the precision of these measurements.

1. V. Punjabi *et al.*, *Eur. Phys. J. A* **51** (2015) 79.
2. S. Pacetti *et al.*, *Phys. Rept.* **550-551** (2015) 1.
3. M. Ablikim *et al.* (BESIII), *Nucl. Instr. Meth. A* **614** (2010) 345.
4. M. Ablikim *et al.* (BESIII Collaboration), *Phys. Rev. Lett.* **124** (2020) 042001, <https://doi.org/10.1103/PhysRevLett.124.042001>.
5. M. Ablikim *et al.* (BESIII Collaboration), *Phys. Rev. D* **99** (2019) 092002, <https://doi.org/10.1103/PhysRevD.99.092002>.
6. M. Ablikim *et al.* (BESIII Collaboration), *Phys. Lett. B* **817** (2021) 136328, <https://doi.org/10.1016/j.physletb.2021.136328>.
7. A. Bianconi, E. Tomasi-Gustafsson, *Phys. Rev. Lett.* **114**, (2015) 232301.
8. A. Bianconi, E. Tomasi-Gustafsson, *Phys. Rev. C* **93** (2016) 035201.
9. T. Lorenz *et al.*, *Phys. Rev. D* **92** (2015) 034018;
10. A. Antonelli *et al.* (FENICE Collaboration), *Nucl. Phys. B* **517** (1998) 3, [https://doi.org/10.1016/S0550-3213\(98\)00083-2](https://doi.org/10.1016/S0550-3213(98)00083-2).
11. D. Bisello *et al.* (DM2 Collaboration), *ZPC* **48** (1990) 2.
12. M. N. Achasov *et al.*, *Phys. Rev. D* **90** (2014) 112007, <https://doi.org/10.1103/PhysRevD.90.112007>; V. P. Druzhinin, S. I. Serednyakov, *EPJ Web Conf.* **212** (2019) 07007, <https://doi.org/10.1051/epjconf/201921207007>.
13. M. Ablikim *et al.* (BESIII Collaboration), *Nat. Phys.* **17** (2021) 12001204, <https://doi.org/10.1038/s41567-021-01345-6>.
14. J. P. Lees *et al.* (BABAR Collaboration), *Phys. Rev. D* **88** (2013) 032011, <https://doi.org/10.1103/PhysRevD.88.032011>.